Accepted Manuscript

Please cite this article as: Outeiriño, D., Costa-Trigo, I., Paz, A., Deive, F. J., Rodríguez, A., & Domínguez, J. M. (2019). Biorefining brewery spent grain polysaccharides through biotuning of ionic liquids. *Carbohydrate Polymers*, 203, 265-274. doi:10.1016/j.carbpol.2018.09.042

Link to published version: https://doi.org/10.1016/j.carbpol.2018.09.042

Biorefining brewery spent grain polysaccharides through biotuning of ionic liquids

David Outeiriño[1], Iván Costa-Trigo[1], Alicia Paz[1], Francisco J. Deive[2], Ana Rodríguez[2], José Manuel Domínguez[1,*]

[1]Industrial Biotechnology and Environmental Engineering Group "*BiotecnIA*", Chemical Engineering Department, University of Vigo (Campus Ourense), 32004 Ourense, Spain

[2]Department of Chemical Engineering, University of Vigo, Edificio Isaac Newton-Campus Lagoas Marcosende, 36310 Vigo, Spain

*Corresponding author: Phone: 34-988-387416, Fax: 34-988-387001, E-mail: jmanuel@uvigo.es

Keywords: *Brewery spent grain; Delignification; Ionic liquids; Cholinium amino acids; Enzymatic hydrolysis*

Abstract

Brewery spent grain (BSG), a relevant waste from beer industry mainly composed of polysaccharides and lignin, is experiencing a surge in the production with its associated environmental impact. Thus, this manuscript bets in the application of aqueous solutions of a cholinium-based ionic liquid (IL) containing glycinate as anion ([N_{1112OH}][Gly]) for an efficient delignification pretreatment. The operation at 90ºC yielded drastic lignin reduction (75.89%), greater than the levels attained when a traditional imidazolium-based IL (1-ethyl-3-methylimidazolium acetate, [C_2C_1im][C_1COO]), was used (40.18%). The advantages of this pretreatment positively impacted the subsequent saccharification reaction, as the levels were increased up to about 1.5 times regarding the control (no IL) or the imidazolium-based pretreatment. ATR-FTIR spectrometry and scanning electron microscopy turned out to be

useful tools to monitor the structural changes exerted. The results presented in this work make up the basis for a rational design of bio-ILs for delignification of lignocellulosic materials.

1. **Introduction**

During the elaboration of beer, highly useful derivatives are also obtained, including brewery spent grain (BSG), the lignocellulosic solid matter resulting from the filtering of wort obtained after the saccharification of the malted cereal grains (generally barley). Spain, with 36.469,219 hectoliters in 2016, is the fourth EU beer producer and the eleventh worldwide, which involves 600,000 tons of BSG/year (Ministerio de Agricultura y Pesca Alimentación y Medio Ambiente;, 2016). The cell walls of BSG are opened to be hydrolyzed into sugars that could be employed as precursor of other added-value compounds or enzymes by microbial transformation (Mussatto, 2014). These facts underscore the potential of this byproduct, usually considered as a waste, to be used as a raw material in biorefinery processes.

Although thermal or chemical hydrolytic processes have been conventionally proposed to obtain sugars (pentoses and hexoses) from lignocellulosic biomass, Green Chemistry principles have urged the scientific community to invest more research efforts in the design of more sustainable strategies. In this scene, an ionic liquid (IL) pretreatment followed by an enzyme-catalyzed hydrolysis could be an appealing option. 1-ethyl-3-methylimidazolium acetate [C_2C_1im][C_1COO] has already been considered the most effective IL for biomass pretreatment as it efficiently solubilize and alters the crystalline structure of cellulose and/or removes lignin, therefore increasing significantly the polysaccharides accessibility to enzymes and consequently improving the enzymatic hydrolysis (Chatel & Rogers, 2014; De Andrade Neto, De Souza Cabral, De Oliveira, Torres, & Morandim-Giannetti, 2016; Parveen, Patra, & Upadhyayula, 2016). Currently, this imidazolium family is the most important one in terms of sales, as the annual production of some of them exceeds the ton magnitude, and they were selected for improving existing industrial processes (e.g. BASIL, aluminum plating; Degussa, paint additives, Pionics, batteries) (Plechkova & Seddon, 2008).

Nonetheless, although the negligible volatility of ILs is an asset to compete with conventional volatile solvents, their high stability and solubility in water could turn them into persistent pollutants if they are discharged/spilled on soils or aquatic environment (Deive et al., 2011). In fact, ILs consisting of imidazolium or pyridinium cations and halide-containing anions have already been demonstrated to be the families bearing more toxicity and environmental persistence (Petkovic, Seddon, Rebelo, & Silva Pereira, 2011), which together with their cost is still limiting their extensive application in different fields.

Accordingly, the production of non-toxic and environmentally friendly ILs from renewable materials is currently in the limelight (Liu, Hou, Li, & Zong, 2012), and their use for separation and environmental processes and biomass biorefining has been proposed (Álvarez et al., 2016; Dutta et al., 2017, 2018; Papa et al., 2017; Xavier et al., 2017; J.-K. Xu, Sun, Xu, & Sun, 2013).In this context, our group has addressed the design of environmentally friendly cholinium-based ILs (N,N,N-trimethylhydroxyethyl ammonium, $[N_{1112OH)}]^{+}$) (Deive et al., 2015), as the biodegradability, reasonable cost and chemical stability of this cation has already been ensured (Liu et al., 2012; Morandeira et al., 2017). Analogously, Ren, Zong, Wu, & Li, 2016 pointed out the suitable role of these bio-ILs for pretreatment and fractionation of lignocellulosic biomass as they could efficiently dissolve lignin, while being poor solvents for microcrystalline cellulose and xylan.

The starting point of this work was the synthesis of a bio-IL derived from renewable and non-toxic natural material (choline hydroxide as the source for the cation; and one amino acid for the anion) through an economical and green route with water as the unique by-product. The data provided by Dutta et al., (2018) for other lignocellulosic materials (grass, hardwood and softwood) reveal the suitability of a polar aminoacid like lysine as anion, but the hypothesis that an apolar and cheaper aminoacid like glycine could be more suitable for delignification pretreatment is planned due to the apolar character of lignin. This IL was applied for the delignification of BSG at different temperatures and its efficiency as a hydrolytic promoter was compared with that achieved after a conventional imidazolium acetate-based pretreatment. The structural modifications imposed by the IL were analyzed in the light of ATR-FTIR spectra.

2. Materials and methods

2.1. Materials

Brewery spent grain (BSG), with approximately 80% water content, was kindly provided by Letra (Vila Verde, Braga, Portugal). BSG humidity content was reduced in the laboratory in an oven (Celsius 2007, Memmert, Schwabach, Germany) at 50°C for approximately 48 h to prevent microbial contamination during storage.

BSG was pretreated with cholinium glycinate [N_{1112OH}][Gly]. This IL was synthesized following the procedure reported by Deive et al., (2015) and its purity was checked by NMR data (>0.95) and its molecular structure is shown in Table 1a. 1-ethyl-3-methylimidazolium acetate [C_2C_1im][C_1COO], which molecular structure is shown in Table 1b was purchased from Sigma-Aldrich (Steinheim, Germany) (>95% purity). The selected ILs were vacuum-dried at reduced pressure and 50ºC for 3 days, and they were stored in amber glass vials with screw caps.

Table 1. Structure of the selected ILs

	Anion	Cation
1a	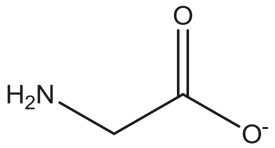 Glycinate	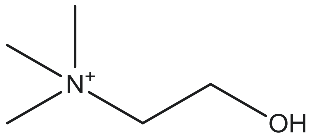 $[N_{1112OH}]^+$
1b	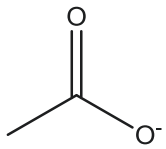 Acetate	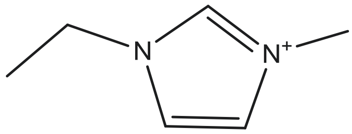 $[C_2C_1im]^+$

Commercial enzyme concentrates *Celluclast 1.5 L* and *Novozym 188*, with cellulase and *β*-glucosidase activities, respectively, were kindly provided by Novozymes, Denmark.

2.2. IL-assisted BSG fractionation.

Ground samples of material (0.5 g) were treated in a 100 mL-glass bottle with 10 g IL (5% w/w) following the methodology reported by Ninomiya et al., (2015) with minor modifications. The mixture was placed into a sand bath, and heated on a hot plate VELP SCIENTIFICA (Usmate Velate, MB, Italy) with vigorous magnetic stirring, in the open atmosphere at 60, 90, 120 or 150ºC for 16 h. Afterwards, the mixture was diluted with 50 mL of acetone/water (1:1 v/v) and stirred for 30 min at room temperature, which resulted in the precipitation of carbohydrate-rich material (CRM), remaining in the liquid phase the lignin-rich material (LRM).

The suspension was centrifuged (Ortoalresa, Consul 21, EBA 20, Hettich Zentrifugen, Germany) at 2755 × g for 30 min, and residual CRM was separated from the supernatant by filtration using a nylon filter. The CRM was washed 4 times with 40 mL water to remove the IL and acetone; and centrifuged under the previously described conditions. The recovered CRM was dried in an oven (Oven Celsius 2007, Memmert, Schwabach, Germany) at 30ºC for 24 h, and gravimetrically measured (Denver Instruments, Bohemia, NY).

Acetone present in liquid phase was evaporated at room temperature causing the precipitation of LRM. After that, it was centrifuged, washed, dried and measured as previously described for CRM.

The streams containing the IL were mixed and vacuum-evaporated in a Büchi rotavapor R-215 (Frankfurt, Germany) at 50ºC, with variable pressure (from 100 to 40 mbar) to ease IL recovery and recycling.

2.3. Characterization of BSG and CRM

Previous to the characterization, BSG was washed with distilled water to avoid the interferences of free sugars from the brewery processes in the analyses. BSG was oven-dried (Binder-Model 53 ED, Tuttlingen, Germany) to constant weight at 105ºC in order to quantify the moisture percentage. Ash content was measured using a muffle furnace (Carbolite ELF 11/6B with controller 301, Derbyshire, United Kingdom) for 6 h at 575ºC. The composition of BSG was determined by quantitative acid hydrolysis (QAH) in two-stages (Pérez-Bibbins, Salgado, Torrado, Aguilar-Uscanga, & Domínguez, 2013). All parameters were performed in triplicate and standard deviations reported in the text.

The CRM was analyzed by QAH following the procedure described by Ninomiya et al., (2015) with slight modifications: 0.1 grams of CRM were treated in a glass test tube with 2 mL sulfuric acid 72% (w/w) for 2 h at room temperature with regular stirring (Ninomiya et al., 2015). Then, samples were diluted with 75 mL of water and autoclaved for 15 min at 121°C. Finally, the two resulting fractions were analyzed as described above.

Glucose, xylose and arabinose were measured by HPLC (Agilent model 1200, Palo Alto, CA) equipped with a refractive index detector and an Aminex HPX-87H ion exclusion column (Bio Rad 300 mm × 7.8 mm, 9 m particles). Elution program with 0.003 M sulfuric acid was at a flow rate of 0.6 mL min^{-1} at 50ºC for 23 minutes.

2.4. Enzymatic hydrolysis

The enzymatic hydrolysis of the raw BSG and the CRMs obtained after pretreatment with $[N_{1112OH}]$[Gly] or $[C_2C_1im][C_1COO]$ with *Celluclast 1.5 L* and *Novozym 188* was assayed in order to evaluate the efficiency of the delignification. The cellulose activity and the *β*-glucosidase activity were ascertained by the filter paper activity test and by spectrophotometric measurements, respectively, following the methodology of Ghose, (1987). The activity was expressed as Filter Paper Units per milliliter (FPU mL^{-1}) and International Units per milliliter (IU mL^{-1}), respectively.

Enzymatic hydrolysis was performed in 250 ml Erlenmeyer flasks using 0.1M sodium citrate buffer (pH 4.85) with liquid-solid ratio 30 g g^{-1} at 48.5ºC and 150 rpm. The enzymatic cocktail tested was cellulase-substrate ratio 28 FPU g^{-1}, and cellobiase-cellulase ratio 13 (IU FPU^{-1}) (Bustos, Moldes, Cruz, & Domínguez, 2005) . Samples were taken at determined times (maximum 72h) and immediately heated for 5 min in boiling water to inactivate the enzymes. Solids were removed by centrifugation at 6000xg for 10 min and filter through 0.2 mm pore membranes (Sartorius, Goettingen, Germany) in order to analyze the concentrations of glucose by HPLC as previously described. All experiments were done in triplicate. Saccharification percentage was calculated as:

$$\%Saccharification = \frac{(Glucose\ released\ \times 0.9)}{Amount\ of\ glucan\ in\ substrate} \times 100$$

2.5. Attenuated Total Reflectance Fourier-transform infrared (ATR-FTIR) spectrometry

Raw BSG, and the CRMs and LRMs fractions obtained after treatment with $[N_{1112OH}]$[Gly] or $[C_2C_1im][C_1COO]$ at 90 °C, were analyzed in triplicate by infrared spectroscopy to check the effectiveness of pretreatments. New and used ILs were also analyzed by the same methodology to check the possibility of reuse the ILs. Infrared spectroscopy measurements were conducted at room temperature in a Thermo Nicolet 6700 FTIR Spectrometer (Thermo Fisher Scientific Inc., Madison, WI, USA), and obtained with an attenuated total reflection ATR accessory equipped with a diamond crystal (Smart Orbit Diamond ATR, Thermo Fisher, USA). Dry samples were recorded without preparation in the range 4000 to 400 cm^{-1} at 4 cm^{-1} resolution and 20 scans using a deuterated triglycine sulfate (DTGS) KBr detector.

2.6. Field Emission Scanning Electron Microscopy (FE-SEM)

The dry samples were mounted onto aluminum stubs and coated with gold in Sputter Coater (Sputtering Emitech K550X, Quorum Technologies, Kent, UK) for 3 min. Finally, samples were observed and photographed in a FE-SEM system (Model JSM-6700F, Jeol, Japan) to study the morphological changes of BSG before and after treatment with $[N_{1112OH}][Gly]$ or $[C_2C_1im][C_1COO]$ at 90ºC.

2.7. Statistical analysis

The average values of the percentage of lignin determined by QAH of raw BSG, as well as the CRMs obtained after treatment with ILs, were subjected to analysis of variance (ANOVA) through a multiple range test with Statgraphics program. Fisher test was used to determine which means are significantly different from others.

3. **Results and discussion**

3.1. Composition of raw bagasse

Aliyu & Bala, (2011) determined that BSG is a material with high nutritive value, containing mainly cellulose, hemicelluloses, lignin and proteins as well as minerals, vitamins and amino acids. Our washed raw material was partially characterized in order to evaluate the influence of IL-treatment on the composition of the main fractions. The characterization compiled in Table 2 shows that polysaccharides (glucan, xylan and arabinan) represent over 50% of the composition of BSG meanwhile Klason and soluble lignin counts on a percentage of 25%.

Table 2. Chemical composition (% dry weight) of raw BSG or CRM obtained after treatment with [N_{1112OH}][Gly] or [C_2C_1im][C_1COO] ILs. All experiments were performed at a solid loading of 5 wt%, during 16h, with vigorous magnetic stirring

Components	**Raw BSG**	**[N_{1112OH}][Gly]**			
		60 ºC	**90 ºC**	**120 ºC**	**150 ºC ***
Humidity	6.38 ± 0.05	10.01 ± 0.60	7.92 ± 0.48	5.19 ± 0.09	4.21
Ashes	4.41 ± 0.22	-	3.45 ± 0.02	-	-
Total Lignin	25.26	12.92	6.09	8.34	13.83
Klason Lignin	17.94 ± 0.30	8.01 ± 0.01	5.01 ± 1.01	6.49 ± 0.48	12.59
Soluble Lignin	7.32 ± 0.02	4.91 ± 0.57	1.08 ± 0.10	1.85 ± 0.06	1.24
Lignin Reduction		48.85	75.89	66.98	45.25
Polysaccharides	52.27	63.30	63.49	67.52	58.57
Glucan	21.84 ± 0.07	30.11 ± 1.07	32.24 ± 0.55	39.78 ± 1.47	49.03
Xylan	21.10 ± 0.07	24.34 ± 0.75	24.18 ± 1.00	22.44 ± 0.40	9.54
Arabinan	9.33 ± 0.19	8.85 ± 0.24	7.07 ± 0.02	5.30 ± 0.20	n.d.
Total	88.33	86.23	81.01	81.07	86.63

*no replicates were obtained since, due to the small amounts recovered, the three samples were joined to allow the analysis. n.d.: not detected

The composition of this material varies depending on the brewing process (including malting and mashing steps), the stage of harvest, the type of cereal or the adjuncts employed (Santos, Jiménez, Bartolomé, Gómez-Cordovés, & del Nozal, 2003). Therefore, literature data (Mussatto & Roberto, 2005, 2006; Russ, Mörtel, & Meyer-Pittroff, 2005) evidence that lignin content may range from 7-8% to 27.8%. Conversely, these authors obtained smaller amounts of glucan (16.8%); meanwhile, (Kanauchi, Mitsuyama, & Araki, 2001) reported up to 25.4%. Hemicelluloses oscillation was smaller, varying between 13.6% xylan and 5.6% arabinan reported by Meneses, Martins, Teixeira, & Mussatto, (2013) to 19.9% and 8.5%, respectively, observed by Mussatto & Roberto, (2006). The high content of polysaccharides and the reduced percentage of lignin postulate BSG as a promising candidate for biorefinery processes to generate fermentable culture media suitable to be converted into bioactive compounds such as bacteriocins or biosurfactants.

3.2. Influence of temperature on [N_{1112OH}][Gly] pretreatment

The election of the IL is a key factor to succeed in the delignification stage, particularly considering that the physical and chemical properties of ILs can be fine-tuned by changing the nature of the anion or cation (J. Sun et al., 2017). Therefore, a judicious selection of the cation and anion will be crucial to create a benign and efficient tailor-made solution (Visser, Swatloski, & Rogers, 2000). In this way, Hou, Xu, Li, & Zong, (2015) stressed the significant lignin solubilizing effect exerted by the anion when 28 cholinium-based ILs were used for the treatment of rice straw. These authors found that the presence of basic groups facilitates the delignification of rice straw, and the use of amino acid-based IL led to increased enzymatic hydrolysis yields than the carboxylate-based counterpart. Consequently, in this work, the role of [N_{1112OH}][Gly] in BSG delignification has been investigated as a prior step to the enzymatic hydrolysis of the cellulosic fraction. The use of this IL avoids the risen concerns over the potential toxicity and low biodegradability of most of the currently employed commercial ILs. Therefore, the use of natural products, such as amino acids, have the potential to be converted into ILs by green procedures, including ion exchange and/or acid-base reactions (Moriel et al., 2010).

It has been documented that IL-based biomass pretreatment takes place at lower temperatures (80-180ºC) than those relying on steam or hot water, which are around 250ºC. In addition, the use of IL does not require high pressure as steam or supercritical fluid (CO_2) pretreatments (Smuga-Kogut et al., 2017). Therefore, the compositions of the carbohydrate-rich material (CRM) obtained after [N_{1112OH}][Gly] addition at different temperatures (60, 90, 120 and 150ºC) are shown in Table 2. The strongest lignin reduction was obtained when raw BSG was treated with [N_{1112OH}][Gly] at 90ºC since the total lignin was reduced in 75.89% (the Klason lignin from 17.94 ± 0.30% to 5.01 ± 1.02% and the soluble lignin from 7.32 ± 0.03% to 1.08 ± 0.11%). The treatment was less effective at 60ºC and 120ºC, with percentages of total lignin in the CRM fractions of 8.34% and 6.49%, respectively. The worst result was achieved at 150ºC since the Klason lignin was scarcely reduced to 12.59% and only the soluble lignin was considerably reduced. In this case, no replicates were obtained due to difficulties in the recovery of the CRM fractions, probably due to the decomposition of this IL at a temperature of 148°C. This thermal data was proved by Moriel et al., (2010) for different choline hydroxide and amino acid-based ILs: [N_{1112OH}] [Ala] 152ºC; [N_{1112OH}][Gly] 148ºC; [N_{1112OH}][Phe] 166ºC; [N_{1112OH}] [Thr] 171ºC and [N_{1112OH}][His] 128ºC.

With comparative purposes the commercial [C_2C_1im][C_1COO] was also evaluated at 90°C. This IL was selected due to Yáñez, Gómez, Martínez, Gullón, & Alonso, (2014) showed its high ability for dissolving cellulose providing good extractability of lignin when *Acacia dealbata* was pretreated. In this case, the use of [C_2C_1im][C_1COO] hardly influenced the Klason lignin (reduction to 11.23 ± 0.86%) and soluble lignin (reduction to 3.88 ± 0.77%)

and a total lignin removal of only 40.18% was recorded, almost half the value achieved under the optimized conditions for the another IL.

The percentages of Klason and soluble lignin removed during the treatments were analyzed by ANOVA and multiple range tests in order to verify the significance of the experiments. Table 3 summarizes the significant differences between raw BSG and all the treatments performed, as well as between the treatments themselves. Regarding Klason lignin, raw BSG showed significant differences ($p<0.05$) for the CRMs obtained after [N_{1112OH}][Gly]-based treatments at different temperatures. It is necessary to point out that the aminoacid-based IL at 90ºC led to the best results and no significant differences were observed at 120ºC, meaning that the optimal range of temperatures is between 90 and 120ºC. This fact is advantageous since the values are lower to the optimal temperatures reported by other authors (Smuga-Kogut et al., 2017). Also of note is that conversely to the expected, in spite of the poor delignification attained with the commercial IL [C_2C_1im][C_1COO], there was also significant difference ($p<0.05$) between raw BSG and the CRM obtained after treatment.

On the other hand, regarding the soluble lignin, significant differences ($p<0.05$) were found between raw BGS and the treatments with the selected synthesized and commercial ILs, indicating an effective soluble lignin removal. When comparing the treatments with [N_{1112OH}][Gly] at different temperatures, the statistical treatment showed significant differences between the treatment at 60ºC and those at 90ºC, 120ºC and 150ºC, however, no significant differences were detected when operating at 90°C, 120°C and 150°C, hence, the lowest temperature (90ºC) was also postulated in order to save in utility expenses. The comparison of both Klason and soluble lignin between [N_{1112OH}][Gly] and [C_2C_1im][C_1COO] (both at 90ºC), evidences the existence of significant differences ($p<0.05$), thus confirming the greater effectiveness of [N_{1112OH}][Gly] in the removal of soluble lignin.

Table 3. Significant differences between the starting material (raw BSG) and the pretreatments with IL

	Klason lignin			Soluble lig	
Contrast	**Sig.**	**Difference**	**+/- Limits**	**Sig.**	**Difference**
[N_{1112OH}][Gly] 60 ºC – Raw BSG	*	-9.93	1.95	*	-2.42
[N_{1112OH}][Gly] 90 ºC – Raw BSG	*	-12.93	1.95	*	-6.25
[N_{1112OH}][Gly] 120 ºC - Raw BSG	*	-11.44	1.95	*	-5.48
[N_{1112OH}][Gly] 150 ºC - Raw BSG	*	4.65	2.47	*	-6.09
[N_{1112OH}][Gly] 90 ºC - [C_2C_1im][C_1COO] 90 ºC	*	-6.21	2.14	*	-2.80
[C_2C_1im][C_1COO] - Raw BSG	*	-6.71	1.95	*	-3.45
[N_{1112OH}][Gly] 60 ºC - [N_{1112OH}][Gly] 90 ºC	*	3.00	2.14	*	3.83
[N_{1112OH}][Gly] 60 ºC - [N_{1112OH}][Gly] 120 ºC		1.51	2.14	*	3.05
[N_{1112OH}][Gly] 60 ºC - [N_{1112OH}][Gly] 150 ºC	*	-14.58	2.62	*	3.67
[N_{1112OH}][Gly] 90 ºC - [N_{1112OH}][Gly] 120 ºC		-1.48	2.14		-0.77
[N_{1112OH}][Gly] 90 ºC - [N_{1112OH}][Gly] 150 ºC	*	-17.58	2.62		-0.16
[N_{1112OH}][Gly]120 ºC - [N_{1112OH}][Gly] 150 ºC	*	-16.09	2.62		0.61

*denotes a statistically significant difference.

It is widely recognized that temperature is the most influential variable on this type of delignification processes; however, the optimal temperature varies depending not only on the IL and material used, but also on operational strategies. For instance, Li et al. (Li et al., 2009) attempted to optimize the pretreatment of wheat straw with 1-ethyl-3-methylimidazolium diethyl phosphate in the range 25-150ºC, reporting about 55% of enzymatic hydrolysis after having operated at 130ºC. Yáñez et al., (2014) corroborated that temperature was the most influential variable on the composition of the solids of *Acacia dealbata* pretreated by [C_2C_1im][C_1COO]. These authors achieved the higher cellulose and xylan recoveries (88% and 66%, respectively) under 150ºC and 30 min. Similarly, the same IL was used by Fu, Mazza, & Tamaki, (2010) for triticale straw pretreatment in the range of 70-150ºC, observing that cellulose crystallinity decreased and the content of extracted lignin increased at higher temperatures, therefore improving the efficiency of enzymatic hydrolysis and the yield of reducing sugars. The best results were achieved at 1.5 h and 150ºC. Finally, Pezoa et al., (2010) proposed the use of [C_2C_1im][Cl] at different temperatures (80, 121, 150 and 170°C) for the pretreatment of different materials (wheat, corn, *Eucalyptus* and Lenga residues), observing optimum sugar yields after saccharification of 30-48% when operating at 150°C for 30-60 min.

Conversely, Pinkert, Goeke, Marsh, & Pang, (2011) investigated the extraction of wood lignin from *Pinus radiata* wood flour with 1-butyl-3-methylimidazolium acesulfamate at temperatures ranging from 80 to 143ºC. In general, higher extraction efficiencies were recorded at elevated temperatures and longer extraction times, although the addition of a cosolvent (DMSO) allowed even greater yields at 100ºC and 2h. In a similar way, N. Sun et al., (2009) reported wood dissolution assisted by [C_2C_1im][C_1COO] operating between 80 and 130ºC. They concluded a greater dissolution effect at higher temperature, which paralleled higher levels of cellulose and IL degradation. Consequently, 110ºC was chosen as a compromise for achieving an enhanced dissolution and avoiding the raw materials disruption.

In addition, Table 4 lists the relative masses of fractionated CRM and LRM in experiments performed with synthesized $[N_{1112OH}]$[Gly] or commercial $[C_2C_1im][C_1COO]$, both at 90ºC. $[C_2C_1im][C_1COO]$ led to higher percentages of CRM recovery (43.3%) than $[N_{1112OH}]$[Gly] (32%). However, only 10% of LRM was obtained with the commercial IL, meaning that 46.2% of the original BSG was not recovered in the process. These losses were reduced up to 26.6% when the amino acid-based IL was employed, as demonstrated by the higher percentage of LRM recovered (41.3%). Table 4 also lists representative data concerning the percentages of polysaccharides yielded. Similar percentages of cellulose (PCR) were obtained with both ILs (47.2% with $[N_{1112OH}]$[Gly] and 48.5% with $[C_2C_1im][C_1COO]$). However, 46.8% of xylan (PXnR) and 42.7% of arabinan (PArR) were attained when the commercial $[C_2C_1im][C_1COO]$ was used, which are higher than the values yielded when the synthesized IL was added (36.6% and 24.2%, respectively). This would indicate that most of the original polysaccharides remain in the corresponding CRM fraction when the latter IL was employed.

Table 4. Percentages of recovery in experiments performed with synthesized [N_{1112OH}][Gly] or commercial [C_2C_1im][C_1COO] at 90ºC, during 16h, and a solid loading of 5 wt%.

	[N_{1112OH}][Gly]	[C_2C_1im][C_1COO]
CRM	32.0	43.3
LRM	41.3	10.0
Losses	26.6	46.2
PCR	47.2	48.5
PXnR	36.6	46.8
PArR	24.2	42.7

CRM: carbohydrate-rich material; LRM: lignin-rich material; PCR: percentage of cellulose recovery; PXnR: percentage of xylan recovery; PArR: percentage of arabinan recovery.

3.3. ATR-FTIR spectra of fractions obtained after pretreatment with [N_{1112OH}][Gly]

Fourier-transform infrared (FTIR) has been widely employed to study either the individual components or the structure of biomass (F. Xu, Yu, Tesso, Dowell, & Wang, 2013). Accordingly, FTIR spectrometry was applied to compare the chemical structure of the original raw material (BSG) with those fractions (CRM and LRM) obtained after the [N_{1112OH}][Gly] or [C_2C_1im][C_1COO] delignification pretreatments at 90 °C. This analysis will consequently allow corroborating the fractionation results observed in Table 2. Among the existing techniques that can be employed to obtain FTIR spectra, attenuated total reflectance (ATR) was used to directly analyze the samples, avoiding extra pretreatments. Therefore, in the ATR-FTIR there is an intimate contact between the sample surface and a crystal (diamond in this case) in such manner that the beam travels through the crystal exciting the surface of the sample and recording the wavelengths of the photons emitted by the sample (Stark, Yelle, & Agarwal, 2016).

Figure 1 shows the FTIR spectra of the raw BSG and the fractions of CRM and LRM after delignification with [N_{1112OH}][Gly] or [C_2C_1im][C_1COO] in the region 4000 to 400 cm^{-1}.

Most of the absorption peaks were assigned according to data presented in the literature (Casas, Alonso, Oliet, Rojo, & Rodríguez, 2012; Hou, Li, & Zong, 2013; Labbé et al., 2005; Ninomiya et al., 2015; Stark et al., 2016; F. Xu et al., 2013; J.-K. Xu et al., 2013; Zhou, Jiang, Via, Fasina, & Han, 2015).

Some similarities have been found between the original BSG and the CRM obtained with [N_{1112OH}][Gly] (Figure 1a) in the range 1741 to 896 cm^{-1} regarding cellulose and hemicellulose content. For instance: the wavenumber 1730 cm^{-1} has been assigned to C=O stretching vibration in acetyl groups on hemicelluloses (Labbé et al., 2005); 1380 cm^{-1} to C-H bending vibration in cellulose, hemicelluloses and lignin (F. Xu et al., 2013); 1240 cm^{-1} to syringyl ring and C-O stretching vibration in lignin, xylan and ester groups (Labbé et al., 2005); 1153 cm^{-1} to C-O-C antisymmetric bridge stretching vibration in cellulose and hemicellulose (Labbé et al., 2005; F. Xu et al., 2013); the prominent signal observed around 1029 to 1024 cm^{-}1 to C-O or C-C in cellulose and hemicelluloses (Zhou et al., 2015); and 898 to 896 cm^{-1} to C-H bending vibrations in cellulose (Labbé et al., 2005) or cellulose and hemicelluloses (Ninomiya et al., 2015).

As expected, these peaks were not detected in the LRM fraction. On the contrary, the characteristic peaks associated with lignin can be observed, mainly in the fingerprint region of 1500 to 400 cm^{-1}, with a higher intensity at 1496 cm^{-1}, which corresponds to aromatic ring vibration in lignin (F. Xu et al., 2013), 1442 cm^{-1} assigned to OH in plane bending in cellulose, hemicellulose or lignin (F. Xu et al., 2013), 1330 cm^{-1} ascribed to syringyl unit breathing with C=O stretching vibration and condensed guaiacyl unit (Casas et al., 2012; Ninomiya et al., 2015; Zhou et al., 2015), 1129 cm^{-1} (ether -O-) (Casas et al., 2012; Ninomiya et al., 2015), 1033 cm^{-1} corresponding to aromatic CH in plane deformation plus CO deformation in primary alcohols plus C=O stretch (unconjugated) (Casas et al., 2012; Ninomiya et al., 2015; Zhou et al., 2015), and 908 cm^{-1} belonging to CH deformation out of plane and aromatic ring (Stark et al., 2016). In addition, some peaks of lower intensity were detected in the region between 700 and 500 cm^{-1}, which indicates the presence of different aromatic compounds and organic halides.

It can also be seen overlapping peaks, making it difficult their identification, in the region between 3200 and 2100 cm^{-1}, with stretching vibrations at media and strong intensities. In particular, the peaks detected between 3200 - 3000 cm^{-1} are indicative of aromatic CH bonds, which is confirmed with strong absorption peaks obtained in the region 1600 - 1400 cm^{-1} (C=C aromatic), 3000 - 2800 cm^{-1} (CH alkanes and alkyl groups), 2850 - 2750 cm^{-1} (C-aldehydes), and 2100 cm^{-1} (C≡C alkyne).

On the other hand, the comparison of the three samples (BSG, CRM and LRM) reveals that most of the lignin present in the original BSG was transferred to the LRM fraction, although residual lignin is still present in the CRM fraction after delignification. Therefore, the peaks present in the regions 2938 and 2885 cm^{-1}, corresponding to CH stretching vibrations of methyl and methylene groups (Stark et al., 2016) and 1600 - 1500 cm^{-1}, belonging to C=C stretching vibration in lignin (Labbé et al., 2005) show higher intensity in the LRM fraction and high to medium in the BSG. However, a peak with less intensity at 2919 cm^{-1} is appreciated in the CRM, which may be indicative of the presence of residual lignin, which would correspond to the data obtained in the QAH shown in Table 2 (5.01 ± 1.017% of Klason lignin). The peak 1741 cm^{-1} can be attributed to C=O stretching due to ester linkages between carbohydrate and lignin (Xie, Hse, Shupe, & Hu, 2015). This peak was detected in the raw BSG and disappeared in CRM and LRM fractions after treatment with the synthesized IL, which suggests the rupture of this bond due to the efficiency of the treatment assayed, and therefore the separation of carbohydrates from lignin.

In general, the analysis of the peaks in the CRM fraction indicates the absence of appreciable amounts of lignin. In the same way, cellulose and hemicelluloses-associated peaks are not present in the LRM fraction. Therefore, the FTIR analysis supports the promising results obtained from the pretreatment of BSG with the [N_{1112OH}][Gly], thus corroborating the efficiency of this delignification pretreatment.

3.4. ATR-FTIR spectra of fractions obtained after pretreatment with [C_2C_1im][C_1COO]

Figure 1b shows the FTIR spectra of the original BSG and CRM and LRM fractions obtained after [C_2C_1im][C_1COO]-based pretreatment. Characteristic peaks associated with carbohydrates (cellulose and hemicelluloses) were observed in the fractionated CRM at 1241 cm^{-1} (syringyl ring and C-O stretching vibration in lignin, xylan and ester groups) (Labbé et al., 2005), 1151 cm^{-1} (C-O-C antisymmetric bridge stretching vibration in cellulose and hemicelluloses) (Zhou et al., 2015), 1022 cm^{-1} (C-O or C-C from cellulose and hemicelluloses) (Zhou et al., 2015) and 896 cm^{-1} (C-H bending vibration in cellulose) (Labbé et al., 2005; Ninomiya et al., 2015).

Meanwhile, characteristic peaks of lignin have also been identified at 2923 cm^{-1} (C-H stretch in methyl and methylene groups on lignin) (Stark et al., 2016), 2854 cm^{-1} (C-H stretch O-CH_3 group) (Stark et al., 2016), 1650 cm^{-1} (C-O stretching vibration in lignin) (Labbé et al., 2005), from 1600 to 1500 cm^{-1} (C=C stretching vibration in lignin) (Labbé et al., 2005), 1454 cm^{-1} (asymetric bending in CH_3 lignin) (Labbé et al., 2005; Ninomiya et al., 2015) y which indicates a non-effective delignification using this IL.

On the other hand, the analysis of the LRM fraction suggests the presence of the characteristic peaks of lignin at 1600 - 1500 cm^{-1} (C=C stretching vibration in lignin) (Labbé et al., 2005), 1452 cm^{-1} (asymmetric bending vibration of CH_3 in lignin) (Labbé et al., 2005; Ninomiya et al., 2015), 919 cm^{-1} (CH deformation of out of plane aromatic ring) (Stark et al., 2016), meaning that the LRM fraction is mainly constituted by lignin, although the reduction in Klason lignin is not significant (from 12.37 ± 0.194 to 11.23 ± 0.864%).

The low efficiency in the delignification stage under this IL is also corroborated by the coincident lignin-associated peaks detected in the three samples (BSG, CRM and LRM). Thus, similar peaks can be observed in the three samples at 1737 cm^{-1} (C=O stretching vibration in lignin (Casas et al., 2012; Zhou et al., 2015) or C=O stretching due to ester linkage between carbohydrate and lignin (Xie et al., 2015) , 2923 cm^{-1} (CH stretch methyl and methylene groups) (Stark et al., 2016), 2852 cm^{-1} (CH stretch $O\text{-}CH_3$ groups) (Stark et al., 2016), and, to a lesser extent, peaks associated with cellulose and hemicellulose at 1241 cm^{-1} (syringyl ring and CO stretching vibration in lignin, xylan and ester groups) (Labbé et al., 2005) and other peaks such as 1168 cm^{-1} (C-O-C ethers).

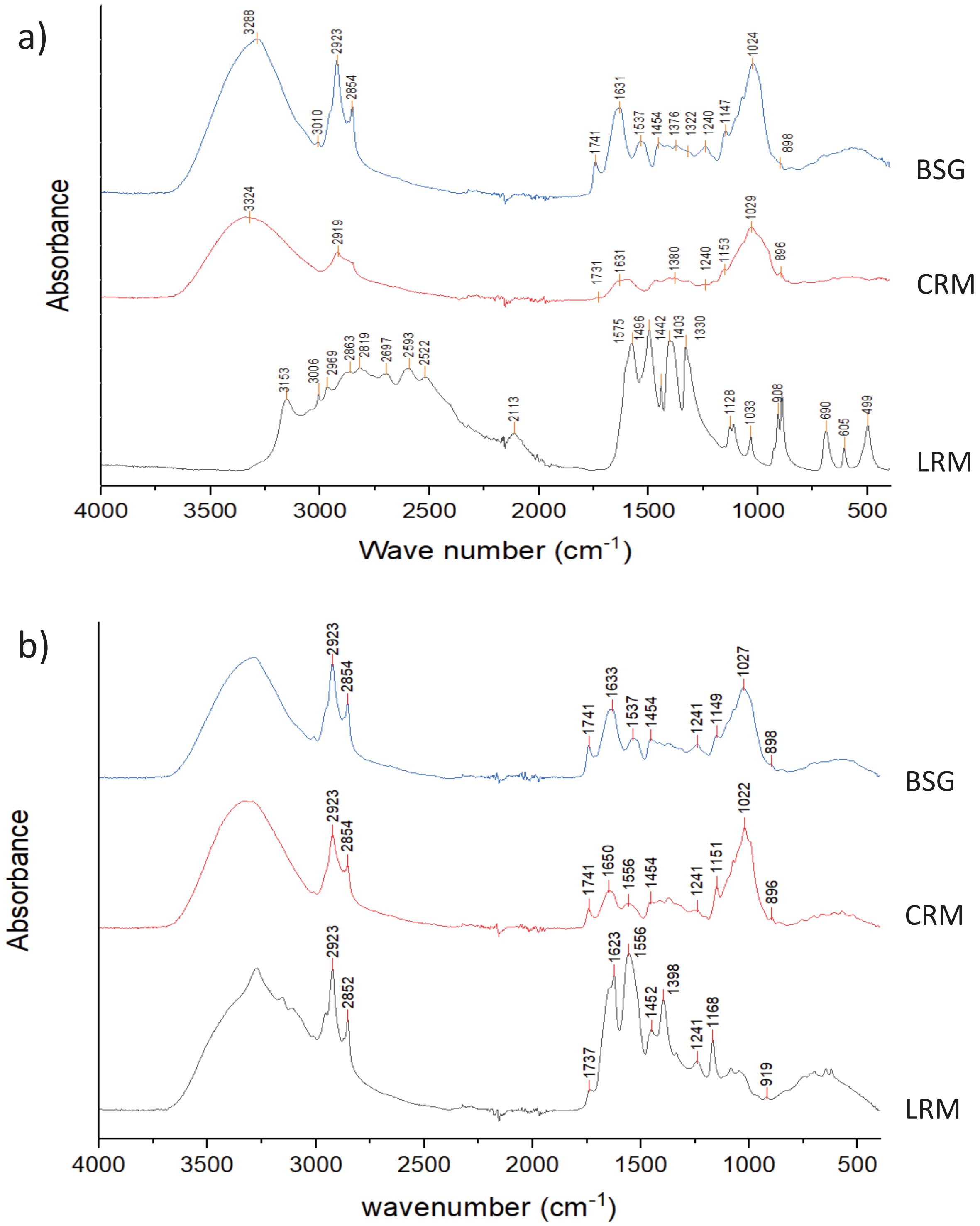

Figure 1. FTIR spectra of raw BSG and cellulosic and lignin materials fractionated with a) 5% (w/w) [N_{1112OH}][Gly] at 90ºC for 16h and b) 5% (w/w) [C_2C_1im][C_1COO] at 90ºC for 16h. BSG: brewery spent grain; CRM: carbohydrate-rich material; LRM: lignin-rich material.

3.5. ATR-FTIR spectra of the recycled ILs

Taking into account the cost associated with the IL synthesis, its recovery and recycling is a key factor for industrial utilization in the light of environmental and economic concerns. Consequently, the IL was submitted to vacuum evaporation at 50ºC, at a pressure varying from 100 to 40 mbar, and it was analyzed by ATR-FTIR.

Raw BSG shows a peak at 1631 cm^{-1} (Figure 1). According to Zhou et al. (Zhou et al., 2015) this peak corresponds to the extracts of the original material. This peak is observed with less intensity in the CRM fraction and disappears in the LRM fraction obtained after pretreatment with [N_{1112OH}][Gly] (Figure 1a). This information suggests that extractives were dissolved into the IL and more research is needed to allow its further reutilization.

Conversely, when the commercial [C_2C_1im][C_1COO] was used, the peak located at 1631 cm^{-1} was clearly identified in the LRM fraction (as 1623 cm^{-1}), while disappearing in the CRM (Figure 1b), suggesting that the IL is free of extracts and could be reused.

These speculations were corroborated with the FTIR spectra of both original and treated ILs (Figure 2), as both ILs did not contain extractives before use. There was no meaningful differences between the FTIR spectra of fresh and recovered [C_2C_1im][C_1COO], showing as the overall chemical structure was maintained under the experimental conditions assayed. Furthermore, the inefficiency of the treatment with [C_2C_1im][C_1COO] was endorsed with the inability to recover also the extractives, being therefore apparently ready to be reused (Figure 2b). However, [N_{1112OH}][Gly] contained this peak (Figure 2a) showing as the extractives were transferred to this IL during the treatment. Consequently, a conditioning step would be required for new uses of this IL.

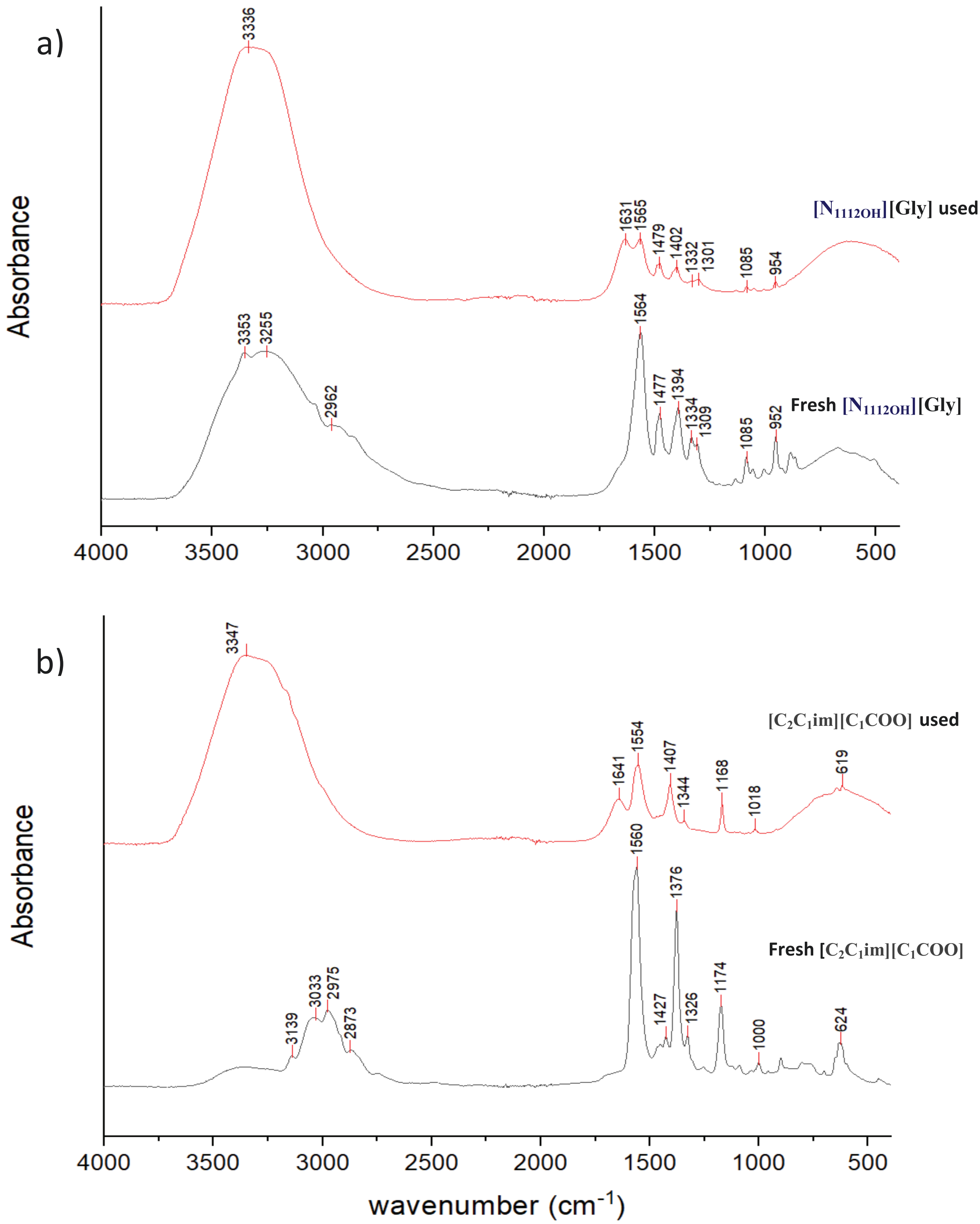

Figure 2. FTIR spectra of a) crude or used $[N_{1112OH}][Gly]$ and b) raw or used $[C_2C_1im][C_1COO]$.

3.6. Enzymatic hydrolysis

A new set of experiments was carried out to study the susceptibility of raw and treated BSG to enzymatic hydrolysis. Figure 3 shows the time course of glucose released from raw BSG or BSG treated with 5% w/w [N_{1112OH}][Gly] or [C_2C_1im][C_1COO] at 90ºC for 16 h. Starting with the raw BSG, the concentration of glucose released upon enzymatic hydrolysis was only 5.58 ± 0.52 g L^{-1} after 72 h, which represented a percentage of saccharification of 59.52%. A similar value of 62.96%, corresponding to 5.63 ± 0.46 g L^{-1} of glucose, was achieved from the [C_2C_1im][C_1COO]-pretreated BSG, demonstrating the inefficiency of this delignification process. However, the efficiency of the [N_{1112OH}][Gly]-assisted delignification of BSG was corroborated by the values of released glucose (13.32 ± 0.80 g L^{-1}), which are about 2.4-fold higher than the control in the absence of IL. This is reflected in the increase of the percentage of saccharification up to 94.25%. It becomes evident that the reduction of the lignin content upon pretreatment shown in Table 2 might contribute to the higher enzymatic hydrolysis efficiency. Lignin content is one of the most notorious substrate features that significantly restricts polysaccharide accessibility to enzymes (Soudham et al., 2015). It was reported that lignin not only acted as a physical barrier in the enzymatic hydrolysis of lignocellulosic biomass, but also was able to non-productively adsorb and even deactivate enzymes. Therefore, its removal would facilitate the enzymatic hydrolysis of the biomass (An, Zong, Hu, & Li, 2017). ILs could be a tool to remove this barrier, increasing the accessibility of cellulases and β-glucosidases used in this work (J. Sun et al., 2017). In particular, the improvement in enzymatic hydrolysis of polysaccharides after pretreatment with the proposed biocompatible IL would mainly stem from extensive and selective delignification (Hou et al., 2015).

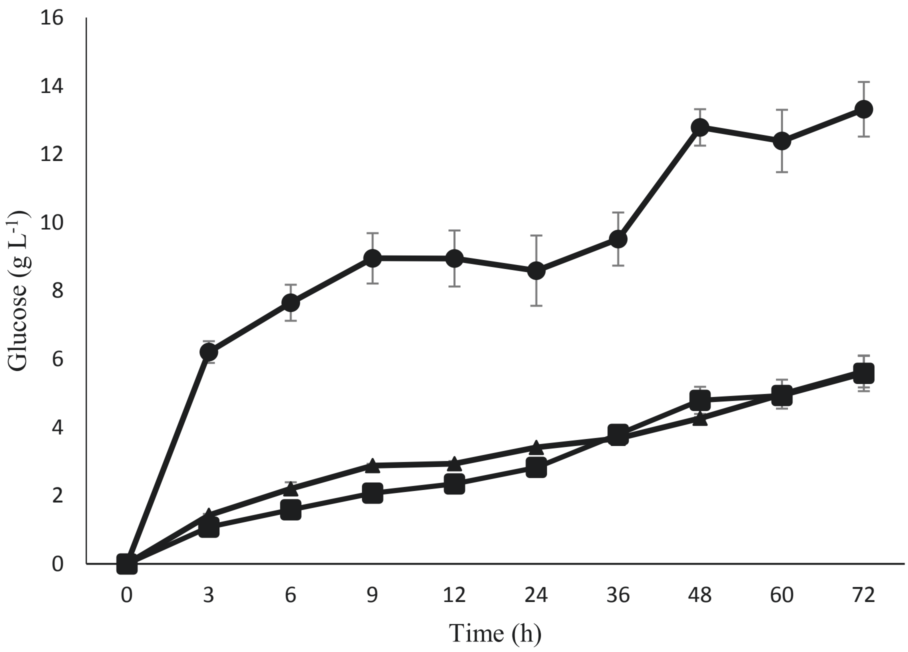

Figure 3. Time courses for enzymatic hydrolysis of raw BSG (■); BSG treated with 5% (w/w) [N_{1112OH}][Gly] at 90ºC for 16h (●), and BSG treated with 5% (w/w) [C_2C_1im][C_1COO] at 90ºC for 16h (▲).

3.7. Scanning electron microscopy

Finally, the changes in the cell walls of raw BSG and CRMs obtained after ILs pretreatment (90ºC, 16 h, and solid loading of 5 wt%) with [N_{1112OH}][Gly] or [C_2C_1im][C_1COO] were observed by SEM images taken at 150 or 300 x magnification (Figure 4). The fiber present in raw BSG, along with the non-fibrous components (hemicellulose and lignin), form a compact structure, considering that lignin and hemicelluloses in plant cells are deposited between the cellulosic microfibrils, therefore becoming an interrupted lamellar structure (Figure 4a). The pretreatment with [N_{1112OH}][Gly] significantly alters the fibrillar structure, removing some of these non-cellulosic components around the fiber bundles (mainly dissolving lignin), thus enabling the microfibrils visualization (Figure 4b). Some lignin or lignin carbohydrate complexes could be condensed on the surface of cellulose fibers (Zhu et al., 2009). However, the pretreatment with [C_2C_1im][C_1COO] was less efficient since the cellulosic microfibrils can be hardly visualized, showing a structure close to the raw material (Figure 4b). This observation corroborates the results of lignin removal compiled in Table 2, as well as the higher efficiency in the enzymatic hydrolysis and higher glucose released in BSG pretreated with [N_{1112OH}][Gly].

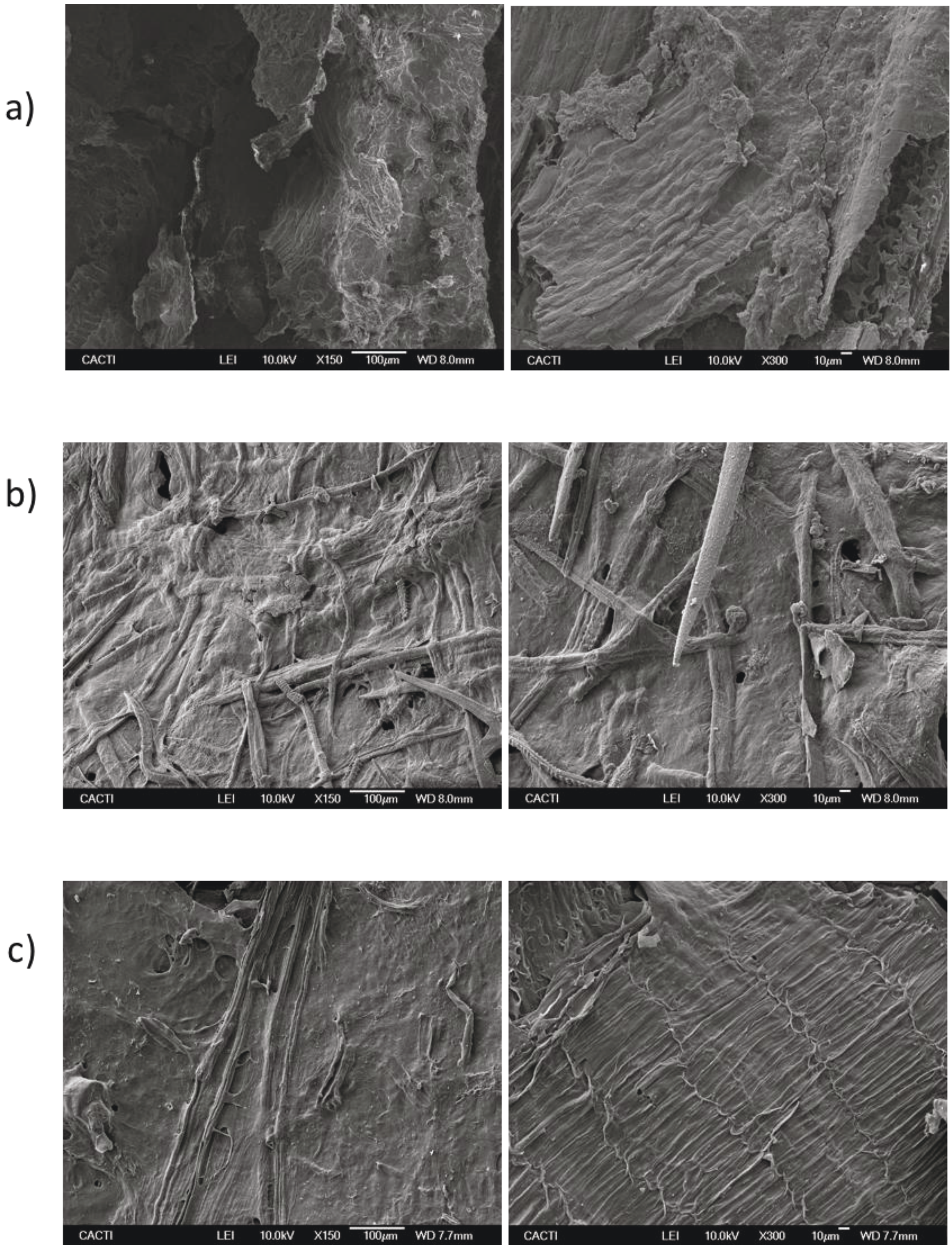

Figure 4. SEM photographs showing the morphology of lignocellulosic surface of a) raw BSG; and CRMs obtained after treatment (90ºC, 16h, and solid loading of 5 wt%) with b) $[N_{1112OH}][Gly]$ or c) $[C_2C_1im][C_1COO]$.

4. **Conclusions**

The valorization of a relevant waste like BSG can be clearly achieved by the use of biocompatible ILs like cholinium-glycinate. The delignification was favored in the presence of this IL at lower temperatures than those required under other current alternatives (e.g. hydrothermal liquefaction, pyrolysis, etc.). The fractionated CRM mostly contained polysaccharides allowing increasing the saccharification efficiency. The removal of lignin paralleled structural changes, as observed by ATR-FTIR spectrometry and scanning electron microscopy. Therefore, this paper demonstrates the appropriateness of cholinium glycinate to improve the lignocellulosic biomass delignification and its subsequent saccharification for a competitive BSG waste biorefinery.

Acknowledgements

Authors are grateful to the Spanish Ministry of Economy and Competitiveness for the financial support of this work (project CTQ2015-71436-C2-1-R), which has partial financial support from the FEDER funds of the European Union, and the Ramón y Cajal contract; and to the Xunta de Galicia for D. Outeiriño pre-doctoral grant, which has partial financial support from the FSE funds. The authors thank Novozymes for the gift of the enzymatic cocktails used in this work. F.J. Deive acknowledges Xunta de Galicia for funding through ED431F 2016/007 project.

References

Aliyu, S., & Bala, M. (2011). Brewer’s spent grain: A review of its potentials and applications. *African Journal of Biotechnology*, *10*(3), 324–331.

Álvarez, M. S., Gómez, L., Ulloa, R. G., Deive, F. J., Sanromán, M. A., & Rodríguez, A. (2016). Antibiotics in swine husbandry effluents: Laying the foundations for their efficient removal with a biocompatible ionic liquid. *Chemical Engineering Journal*, *298*, 10–16.

An, Y.-X., Zong, M.-H., Hu, S.-Q., & Li, N. (2017). Effect of residual lignins present in cholinium ionic liquid-pretreated rice straw on the enzymatic hydrolysis of cellulose. *Chemical Engineering Science*, *161*, 48–56.

Bustos, G., Moldes, A. B., Cruz, J. M., & Domínguez, J. M. (2005). Production of lactic acid from vine-trimming wastes and viticulture lees using a simultaneous saccharification fermentation method. *Journal of the Science of Food and Agriculture*, *85*(3), 466–472.

Casas, A., Alonso, M. V., Oliet, M., Rojo, E., & Rodríguez, F. (2012). FTIR analysis of lignin regenerated from Pinus radiata and Eucalyptus globulus woods dissolved in imidazolium-based ionic liquids. *Journal of Chemical Technology and Biotechnology*, *87*(4), 472–480.

Chatel, G., & Rogers, R. D. (2014). Review: Oxidation of lignin using ionic liquids-an innovative strategy to produce renewable chemicals. *ACS Sustainable Chemistry and Engineering*, *2*(3), 322–339.

De Andrade Neto, J. C., De Souza Cabral, A., De Oliveira, L. R. D., Torres, R. B., & Morandim-Giannetti, A. D. A. (2016). Synthesis and characterization of new low-cost ILs based on butylammonium cation and application to lignocellulose hydrolysis. *Carbohydrate Polymers*, *143*, 279–287.

Deive, F. J., Rodríguez, A., Varela, A., Rodrígues, C., Leitão, M. C., Houbraken, J. A. M. P., … Silva Pereira, C. (2011). Impact of ionic liquids on extreme microbial biotypes from soil. *Green Chemistry*, *13*(3), 687.

Deive, F. J., Ruivo, D., Rodrigues, J. V., Gomes, C. M., Sanromán, M. Á., Rebelo, L. P. N., … Rodríguez, A. (2015). On the hunt for truly biocompatible ionic liquids for lipase-catalyzed reactions. *RSC Advances*, *5*(5), 3386–3389.

Dutta, T., Isern, N. G., Sun, J., Wang, E., Hull, S., Cort, J. R., … Singh, S. (2017). Survey of Lignin-Structure Changes and Depolymerization during Ionic Liquid Pretreatment. *ACS Sustainable Chemistry & Engineering*, *5*(11), 10116–10127.

Dutta, T., Papa, G., Wang, E., Sun, J., Isern, N. G., Cort, J. R., … Singh, S. (2018). Characterization of Lignin Streams during Bionic Liquid-Based Pretreatment from Grass, Hardwood, and Softwood. *ACS Sustainable Chemistry & Engineering*, *6*(3), 3079–3090.

Fu, D., Mazza, G., & Tamaki, Y. (2010). Lignin Extraction from Straw by Ionic Liquids and Enzymatic Hydrolysis of the Cellulosic Residues. *Journal of Agricultural and Food Chemistry*, *58*(5), 2915–2922.

Ghose, T. K. (1987). Measurement of cellulase activities. *Pure and Applied Chemistry*, *59*(2), 257–268.

Hou, X.-D., Li, N., & Zong, M.-H. (2013). Renewable bio ionic liquids-water mixtures-mediated selective removal of lignin from rice straw: Visualization of changes in composition and cell wall structure. *Biotechnology and Bioengineering*, *110*(7), 1895–1902.

Hou, X.-D., Xu, J., Li, N., & Zong, M.-H. (2015). Effect of anion structures on cholinium ionic liquids pretreatment of rice straw and the subsequent enzymatic hydrolysis. *Biotechnology and Bioengineering*, *112*(1), 65–73. 5

Kanauchi, O., Mitsuyama, K., & Araki, Y. (2001). Development of a functional germinated barley foodstuff from brewer's spent grain for the treatment of ulcerative colitis. *Journal of the American Society of Brewing Chemists*, *59*(2), 59–62.

Labbé, N., Rials, T., Kelley, S., Cheng, Z. M., Kim, J. Y., & Li, Y. (2005). FT-IR imaging and pyrolysis-molecular beam mass spectrometry: New tools to investigate wood tissues. *Wood Science and Technology*, *39*(1), 61–76.

Li, Q., He, Y.-C., Xian, M., Jun, G., Xu, X., Yang, J.-M., & Li, L.-Z. (2009). Improving enzymatic hydrolysis of wheat straw using ionic liquid 1-ethyl-3-methyl imidazolium diethyl phosphate pretreatment. *Bioresource Technology*, *100*(14), 3570–3575.

Liu, Q.-P., Hou, X.-D., Li, N., & Zong, M.-H. (2012). Ionic liquids from renewable biomaterials: synthesis, characterization and application in the pretreatment of biomass. *Green Chem.*, *14*(2), 304–307.

Meneses, N. G. T., Martins, S., Teixeira, J. A., & Mussatto, S. I. (2013). Influence of extraction solvents on the recovery of antioxidant phenolic compounds from brewer's spent grains. *Separation and Purification Technology*, *108*, 152–158.

Ministerio de Agricultura y Pesca Alimentación y Medio Ambiente; (2016). *Informe socioeconómico del sector de la cerveza en España 2016*. Retrieved from http://publicacionesoficiales.boe.es/

Morandeira, L., Álvarez, M. S., Markiewicz, M., Stolte, S., Rodríguez, A., Sanromán, M. Á., & Deive, F. J. (2017). Testing True Choline Ionic Liquid Biocompatibility from a Biotechnological Standpoint. *ACS Sustainable Chemistry & Engineering*, *5*(9), 8302–8309.

Moriel, P., García-Suárez, E. J., Martínez, M., García, A. B., Montes-Morán, M. A., Calvino-Casilda, V., & Bañares, M. A. (2010). Synthesis, characterization, and catalytic activity of ionic liquids based on biosources. *Tetrahedron Letters*, *51*(37), 4877–4881.

Mussatto, S. I. (2014). Brewer's spent grain: A valuable feedstock for industrial applications. *Journal of the Science of Food and Agriculture*, *94*(7), 1264–1275.

Mussatto, S. I., & Roberto, I. C. (2005). Acid hydrolysis and fermentation of brewer's spent grain to produce xylitol. *Journal of the Science of Food and Agriculture*, *85*(14), 2453–2460.

Mussatto, S. I., & Roberto, I. C. (2006). Chemical characterization and liberation of pentose sugars from brewer's spent grain. *Journal of Chemical Technology and Biotechnology*, *81*(3), 268–274.

Ninomiya, K., Inoue, K., Aomori, Y., Ohnishi, A., Ogino, C., Shimizu, N., & Takahashi, K. (2015). Characterization of fractionated biomass component and recovered ionic liquid during repeated process of cholinium ionic liquid-assisted pretreatment and fractionation. *Chemical Engineering Journal*, *259*, 323–329.

Papa, G., Feldman, T., Sale, K. L., Adani, F., Singh, S., & Simmons, B. A. (2017). Parametric study for the optimization of ionic liquid pretreatment of corn stover. *Bioresource Technology*, *241*, 627–637.

Parveen, F., Patra, T., & Upadhyayula, S. (2016). Hydrolysis of microcrystalline cellulose using functionalized Bronsted acidic ionic liquids - A comparative study. *Carbohydrate Polymers*, *135*, 280–284.

Pérez-Bibbins, B., Salgado, J. M., Torrado, A., Aguilar-Uscanga, M. G., & Domínguez, J. M. (2013). Culture parameters affecting xylitol production by Debaryomyces hansenii immobilized in alginate beads. *Process Biochemistry*, *48*(3), 387–397.

Petkovic, M., Seddon, K. R., Rebelo, L. P. N., & Silva Pereira, C. (2011). Ionic liquids: a pathway to environmental acceptability. *Chem. Soc. Rev.*, *40*(3), 1383–1403.

Pezoa, R., Cortinez, V., Hyvärinen, S., Reunanen, M., Hemming, J., Lienqueo, M. E., … Mikkola, J. P. (2010). Use of ionic liquids in the pretreatment of forest and agricultural residues for the production of bioethanol. *Cellulose Chemistry and Technology*, *44*(4–6), 165–172.

Pinkert, A., Goeke, D. F., Marsh, K. N., & Pang, S. (2011). Extracting wood lignin without dissolving or degrading cellulose: investigations on the use of food additive-derived ionic liquids. *Green Chemistry*, *13*(11), 3124.

Plechkova, N. V., & Seddon, K. R. (2008). Applications of ionic liquids in the chemical industry. *Chem. Soc. Rev.*, *37*(1), 123–150.

Ren, H., Zong, M. H., Wu, H., & Li, N. (2016). Efficient Pretreatment of Wheat Straw Using Novel Renewable Cholinium Ionic Liquids to Improve Enzymatic Saccharification. *Industrial and Engineering Chemistry Research*, *55*(6), 1788–1795.

Russ, W., Mörtel, H., & Meyer-Pittroff, R. (2005). Application of spent grains to increase porosity in bricks. *Construction and Building Materials*, *19*(2), 117–126.

Santos, M., Jiménez, J. ., Bartolomé, B., Gómez-Cordovés, C., & del Nozal, M. . (2003). Variability of brewer's spent grain within a brewery. *Food Chemistry*, *80*(1), 17–21.

Smuga-Kogut, M., Zgórska, K., Kogut, T., Kukiełka, K., Wojdalski, J., Kupczyk, A., … Wielewska, I. (2017). The use of ionic liquid pretreatment of rye straw for bioethanol production. *Fuel*, *191*, 266–274.

Soudham, V. P., Raut, D. G., Anugwom, I., Brandberg, T., Larsson, C., & Mikkola, J.-P. (2015). Coupled enzymatic hydrolysis and ethanol fermentation: ionic liquid pretreatment for enhanced yields. *Biotechnology for Biofuels*, *8*(1), 135.

Stark, N. M., Yelle, D. J., & Agarwal, U. P. (2016). Techniques for Characterizing Lignin. In *Lignin in Polymer Composites* (pp. 49–66). Elsevier.

Sun, J., Konda, N. V. S. N. M., Parthasarathi, R., Dutta, T., Valiev, M., Xu, F., … Singh, S. (2017). One-pot integrated biofuel production using low-cost biocompatible protic ionic liquids. *Green Chemistry*, *19*(13), 3152–3163.

Sun, N., Rahman, M., Qin, Y., Maxim, M. L., Rodríguez, H., & Rogers, R. D. (2009). Complete dissolution and partial delignification of wood in the ionic liquid 1-ethyl-3-methylimidazolium acetate. *Green Chemistry*, *11*(5), 646.

Visser, A. E., Swatloski, R. P., & Rogers, R. D. (2000). pH-Dependent partitioning in room temperature ionic liquids provides a link to traditional solvent extraction behavior. *Green*

Chemistry, *2*(1), 1–4.
Xavier, L., Deive, F. J., Sanromán, M. A., Rodríguez, A., Freire, M. S., González-Álvarez, J., … Ulloa, R. G. (2017). Increasing the Greenness of Lignocellulosic Biomass Biorefining Processes by Means of Biocompatible Separation Strategies. *ACS Sustainable Chemistry & Engineering*, *5*(4), 3339–3345.
Xie, J., Hse, C.-Y., Shupe, T. F., & Hu, T. (2015). Physicochemical characterization of lignin recovered from microwave-assisted delignified lignocellulosic biomass for use in biobased materials. *Journal of Applied Polymer Science*, *132*(40), 42635.
Xu, F., Yu, J., Tesso, T., Dowell, F., & Wang, D. (2013). Qualitative and quantitative analysis of lignocellulosic biomass using infrared techniques: A mini-review. *Applied Energy*, *104*, 801–809.
Xu, J.-K., Sun, Y.-C., Xu, F., & Sun, R.-C. (2013). Characterization of Hemicelluloses Obtained from Partially Delignified Eucalyptus Using Ionic Liquid Pretreatment. *BioResources*, *8*(2), 1946–1962.
Yáñez, R., Gómez, B., Martínez, M., Gullón, B., & Alonso, J. L. (2014). Valorization of an invasive woody species, Acacia dealbata, by means of Ionic liquid pretreatment and enzymatic hydrolysis. *Journal of Chemical Technology & Biotechnology*, *89*(9), 1337–1343.
Zhou, C., Jiang, W., Via, B. K., Fasina, O., & Han, G. (2015). Prediction of mixed hardwood lignin and carbohydrate content using ATR-FTIR and FT-NIR. *Carbohydrate Polymers*, *121*, 336–341.
Zhu, Z., Sathitsuksanoh, N., Vinzant, T., Schell, D. J., McMillan, J. D., & Zhang, Y.-H. P. (2009). Comparative study of corn stover pretreated by dilute acid and cellulose solvent-based lignocellulose fractionation: Enzymatic hydrolysis, supramolecular structure, and substrate accessibility. *Biotechnology and Bioengineering*, *103*(4), 715–724.